The Fermi surface of the most dilute superconductor

Xiao Lin[1,2], Zengwei Zhu[1], Benoît Fauqué[1], and Kamran Behnia[1]

[1] *LPEM (UPMC-CNRS), Ecole Supérieure de Physique et de Chimie Industrielles, 75005 Paris, France*

[2] *Department of Physics, Zhejiang University, Hangzhou, 310027, China*

(Dated: November 13, 2012)

Abstract

$SrTiO_3$ is a large-gap transparent insulator, which upon the introduction of n-type carriers undergoes a superconducting transition below 1 K. Discovered in 1964[1], it has been the first member of a loose family of "semiconducting superconductors"[2], which now includes column-IV elements [3]. Recent attention has focused on the interface between $SrTiO_3$ and other insulators[4] or vacuum[5], a two-dimensional metal with a superconducting ground state[6, 7]. The origin of superconductivity in the bulk system is a mystery, since the non-monotonous variation of the critical temperature with carrier concentration defies the expectations of the most crude version of the BCS theory. Here, employing the Nernst effect, an extremely sensitive probe of tiny bulk Fermi surfaces[8], we show that down to concentrations as low as $5.5 \times 10^{17} cm^{-3}$, the system has both a sharp Fermi surface and a superconducting ground state. The most dilute superconductor currently known has therefore a metallic normal state with a Fermi energy as little as 1.1 meV on top of a band gap as large as 3 eV. The survival of superconductivity at such a low carrier density in presence of a single quasi-spherical Fermi surface puts strong constraints for the identification of the pairing mechanism.

$SrTiO_3$ is a failed ferroelectric with an exceptionally large dielectric constant[9]. This leads to a significant enhancement in the screening length scale. When a dopant is introduced, the Coulomb potential of the excess charge is detectable over a distance much longer than the lattice parameter. According to Mott, in a doped semiconductor, when the average distance between the dopants ($d = n^{-1/3}$) becomes a sizeable fraction of the effective Bohr radius, a_B^*, metal-insulator transition occurs. This Mott criterion for the critical concentration, $n_c^{1/3} a_B^* = 0.26$, has been observed to hold in a wide range of semiconductors[10]. Thanks to its long effective Bohr radius, doped $SrTiO_3$ displays a finite zero-temperature conductivity down to carrier concentrations as low as $n = 8 \times 10^{15} cm^{-3}$ [11]. This is orders of magnitude lower than the the threshold of metallicity in silicon ($3.5 \times 10^{18} cm^{-3}$) or in germanium($3.5 \times 10^{17} cm^{-3}$)[10].

Superconductivity emerges at higher doping levels, when the system is $n-$doped by either of the three possible routes: substituting titanium with niobium[12–14], or strontium with lanthanum[15] or removing oxygen[12]. Intriguingly, the superconducting ground state is restricted to a limited doping window[12–15]. Thanks to the remarkably high mobility of electrons, another consequence of the large dielectric constant[11], quantum oscillations are observable and have been reported both in the bulk[16, 17] and in the two-dimensional[18–20] samples.

Two hitherto unanswered questions are addressed by the present work: i) Is there a threshold in carrier concentration for the emergence of superconductivity? ii) Has the normal state of such a low-density superconductor a well-defined Fermi surface or is it just an impurity-band metal? We attempt to answer these questions by a study of the low-temperature Nernst effect in both oxygen-reduced and Nb-doped $SrTiO_3$ across a wide (i.e. three-orders-of-magnitude) window of carrier density. We find that superconductivity persists down to a carrier concentration significantly lower than what was previously believed. This firmly establishes $n-$doped $SrTiO_3$ as the most dilute known superconductor with a carrier density as low as $5.5 \times 10^{17} cm^{-3}$, which corresponds to the removal of one oxygen atom out of 10^5. Single-frequency quantum oscillations resolved at this doping level identify the normal-state as a metal with a single quasi-spherical Fermi surface.

Fig. 1 presents the variation of the Nernst signal (S_{xy}=E_y/-$\nabla_x T$) as a function of the inverse of the magnetic field for seven samples with different carrier concentrations, kept at the same temperature (0.5 K)[See the supplement for details on sample characterization]. As

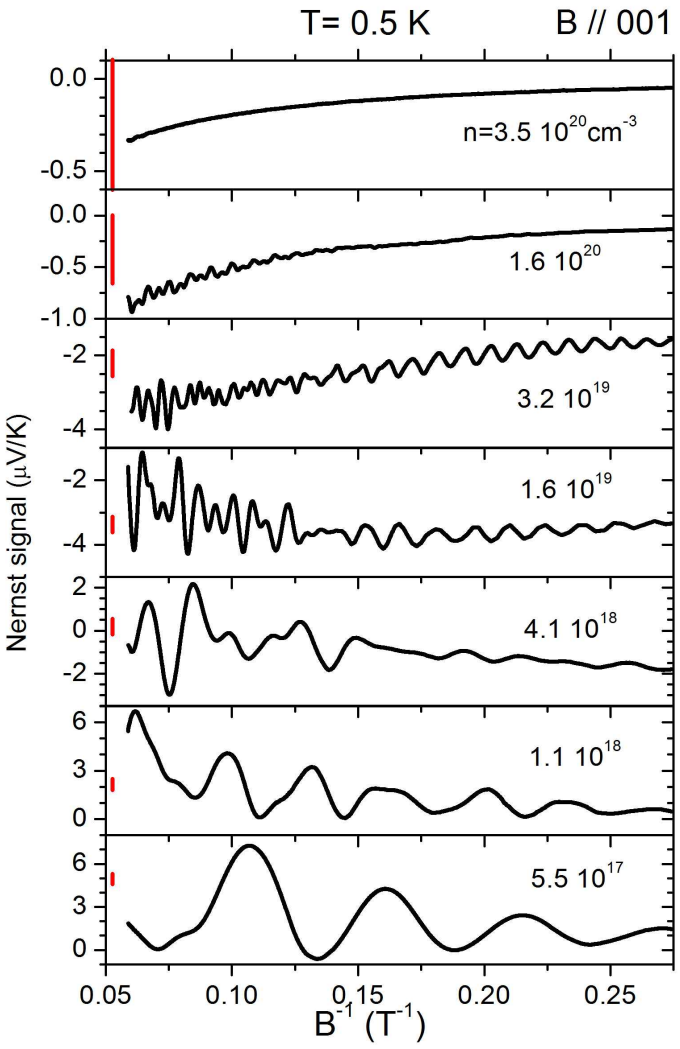

FIG. 1: **Emergence of Nernst quantum oscillations:** As the carrier density is reduced in $SrTiO_3$, the Nernst signal shows oscillations with larger amplitude and longer periodicity. In each panel, the vertical red bar represents a constant scale of 0.7 $\mu V/K$.

seen in the figure, quantum oscillations are barely detectable in the sample with the highest carrier density. As n decreases, the amplitude of oscillations grow while their frequency shrink. Giant oscillations of the Nernst effect with the approach of the quantum limit were previously observed in semimetallic bismuth[21] and graphite[8], as well as doped Bi_2Se_3[22]. A property these three systems share with lightly-doped $SrTiO_3$ is that their Fermi surface is an extremely small portion of the Brillouin zone. A 10 T magnetic field truncates such a tiny Fermi surface in to a few Landau tubes. In such a context, each time a squeezed Landau tube leaves the Fermi surface, the Nernst signal peaks. The Nernst quantum oscillations are

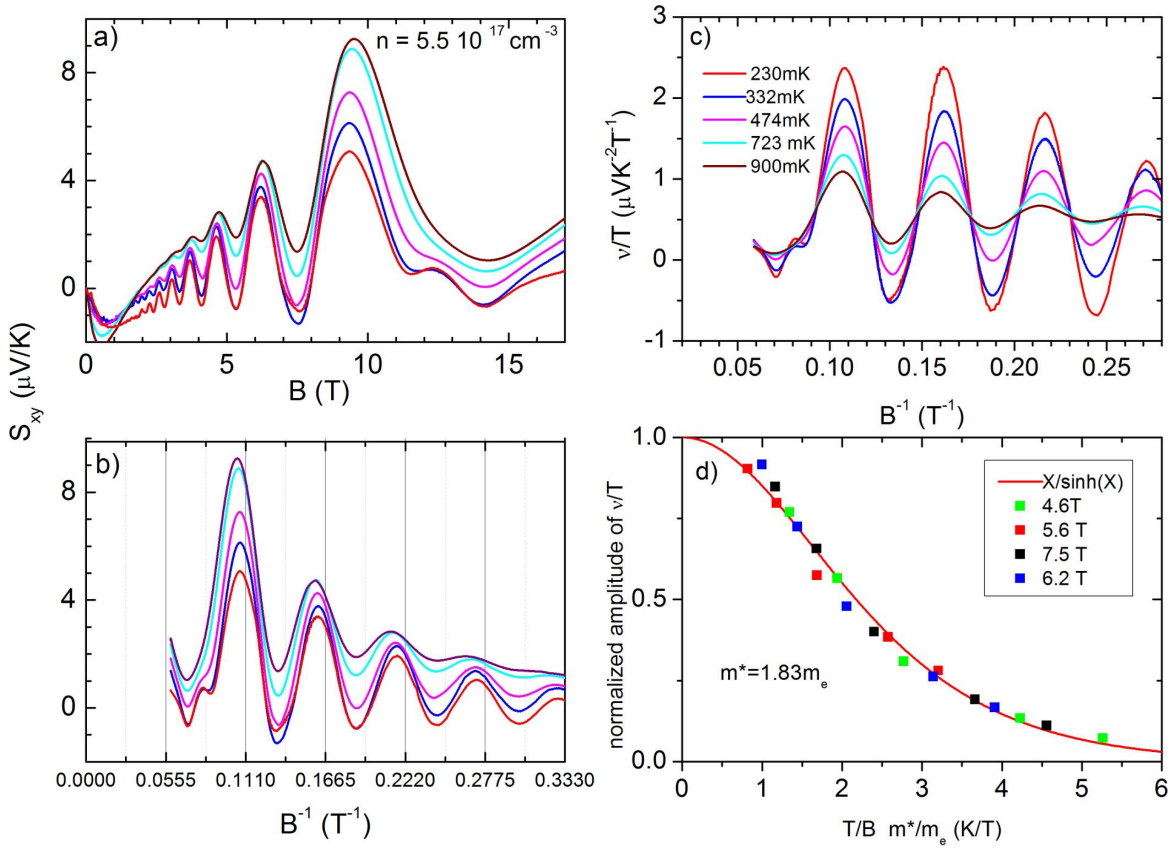

FIG. 2: **A single periodicity at the lowest doping:** Nernst quantum oscillations as a function of magnetic field **(a)** and the inverse of magnetic field **(b)** at different temperatures for the sample with a carrier density of $5.5\times10^{17}cm^{-3}$. There is a single periodicity with the lowest peak displaying Zeeman splitting.**c)**The variation of Nernst coefficient ($\nu = S_{xy}/B$ divided by temperature with the inverse of magnetic field at different temperatures.**d)** The amplitude of oscillations in ν/T, for different magnetic fields and temperatures. Solid line represents the damping expected in the Lifshitz-Kosevitch theory for an effective mass of 1.83.

concomitant with Shubnikov-de Haas osillations. For the lowest Landau indexes, however, while the oscillating component of resistivity is a small fraction of the overall signal, the oscillating part of the Nernst coefficient dominates the monotonous background[8]. This makes the analysis of the Nernst data straightforward.

As seen in Fig. 1, in the intermediate doping range, the oscillations display a complex structure and several frequencies are detectable. For the lowest doping levels, the structure becomes simpler. Fig.2 zooms displays detailed data for the sample at $n_1 = 5.5 \times 10^{17}cm^{-3}$.

As seen in the figure there is a clearly a single periodicity for all temperatures. Moreover, the Nernst peak for the lowest detected Landau level is split at low enough temperatures. The data immediately settles the periodicity ($0.0555T^{-1}$), and subsequently the frequency (18.2 T). The distance between the two spin-split-peaks quantifies the relative magnitudes of the Zeeman(E_z) and cyclotron(E_c) energies . This is the first time that the Zeeman splitting has been clearly detected in the system.

For samples with larger carrier densities ($n \geq 1.05 \times 10^{18} cm^{-3}$), the spectrum of oscillations is significantly more complex, indicative of the presence of more than one component of the Fermi surface [See the supplement]. This is in agreement with the results of recent *ab initio* band calculations[23]. As the insulator is doped by n-type carriers, the first available band to be filled is a threefold degenerate one associated with Ti *3d* orbital. The threefold degeneracy is lifted first by spin-orbit coupling and then by the crystal electric field. Filling these bands successively generates three interpenetrating ellipsoids at the center of the Brillouin zone. Calculations estimate the critical doping to start filling the second band to be $x_{c1} = 4 \times 10^{-5}$ carrier per formula unit[23]. This corresponds to a carrier density of $n_{c1} = 6.8 \times 10^{17} cm^{-3}$, slightly larger than our most dilute sample. Therefore, there is a fair agreement between experiment and theory.

According to the Onsager relation, the frequency of quantum oscillations, F, is set by the extremal cross section of the Fermi surface,A_k: $F = (\frac{\hbar}{2\pi e})A_k$. A frequency of 18.2 T implies a cross section of $A = 0.18 nm^{-2}$. Now, assuming a spherical Fermi surface, this gives a carrier density of $4.6 \times 10^{17} cm^{-3}$, very close to what is given by measuring the Hall resistivity ($n = \frac{1}{eR_H} = 5.5 \times 10^{17}) cm^{-3}$. We conclude that at this concentration, the Fermi surface is a slightly anisotropic sphere. This is again in agreement with the expectations of the band calculations, which do not find sizeable anisotropy in dispersion along [100], [101] and [110] for $n < n_{c1}$.

In the Lifshitz-Kosevitch theory, the thermal smearing of quantum oscillations is set by the magnitude of cyclotron mass, m^*. As the temperature increases, the ratio of thermal energy to the cyclotron energy increases.Therefore the amplitude of oscillations decreases following $\frac{X}{sinhX}$ dependence. Here, X is a dimensionless temperature normalized by magnetic field and effective mass: $X = (\frac{2\pi^2 k_B}{\hbar e})(\frac{m^* T}{B})$. As in the case of Bi_2Se_3[22], we found that employing this formalism to oscillations of the Nernst coefficient divided by temperature (ν/T) (See Fig. 2c) leads to an accurate determination of the cyclotron mass. Fig. 2d,

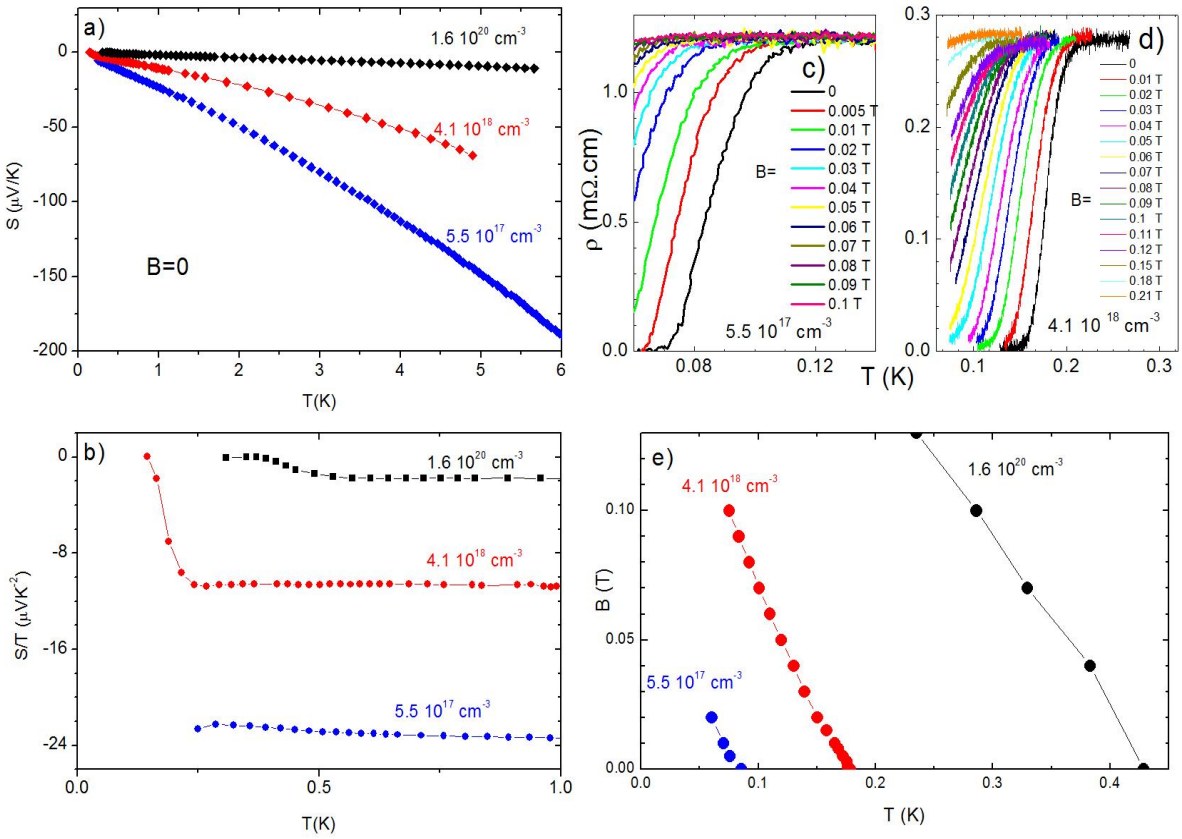

FIG. 3: **Evolution of Fermi temperature and superconducting properties with doping: a)** The temperature dependence of the zero-field Seebeck coefficient at three different dopings. **b)**Temperature dependence of S/T. As seen in the figure, with underdoping, the diffusive component of thermopower becomes larger and larger, indicating a smaller Fermi energy. **c and d)** Superconducting resistive transition for two different carrier concentrations in presence of magnetic field. **e)** Temperature-dependence of the upper critical field near T_c (defined as the temperature at which resistivity drops by half) for three carrier concentrations.

compares the experimentally resolve amplitudes at different field and temperatures with the expectations of equation 1 assuming $m^* = 1.83m_e$. We found that a fit to our Shubnikov- de Haas data yields a quasi-identical value for the effective mass of $m^* = (1.82 \pm 0.05)m_e$ [See the supplement]. This value is in fair agreement with what was obtained by measuring the plasma frequency ($m^* = (2 \pm 0.3)m_e$)[26]. Note, however, that the latter measurements are performed at higher concentrations where several bands with possibly different masses are present. The cyclotron mass obtained here is 2.5 times larger than the the band mass(0.7

m_e[23, 26]), an enhancement caused by a combination of electron-phonon and electron-electron interactions.

The Fermi temperature of this dilute liquid of electrons can be estimated in two distinct ways. First, the magnitude of cyclotron mass together with the size of the Fermi wave-vector k_F obtained from the frequency of the quantum oscillations can be plugged to:

$$k_B T_F = \frac{\hbar^2 k_F^2}{2m^*} \tag{1}$$

to obtain the Fermi temperature. This yields $\mathrm{T}_F = 13.5K$.

Another route to estimate the Fermi temperature is to put under scrutiny the magnitude of the Seebeck coefficient. In a wide variety of correlated metals, the slope of the Seebeck coefficient in the zero-temperature limit is inversely proportional to the Fermi temperature as expected in the semi-classical transport theory for a Fermi liquid[24]. In doped $SrTiO_3$, the magnitude of the Seebeck coefficient in the intermediate temperature range is known to be remarkably large[25]. Panels a and b in Fig. 3 display the evolution of low-temperature Seebeck coefficient in $SrTiO_3$ with doping. As seen in the figure, as the carrier density lowers, the diffusive component of the Seebeck coefficient increases. In the sample with the lowest carrier concentration ($n = 5.5 \times 10^{17} cm^{-3}$) , the magnitude of S/T becomes as large as $-22 \mu V K^{-2}$. Assuming an energy-independent mean-free-path and a spherical Fermi surface, a Fermi temperature of $\mathrm{T}_F = 12.9K$ is obtained using the equation:

$$|\frac{S}{T}| = \frac{\pi^2}{3} \frac{k_B}{e} \frac{1}{T_F} \tag{2}$$

Thus, data obtained from two independent probes converge to a Fermi temperature as low as 13 K. The energy gap between valence and conduction bands in $SrTiO_3$ is as large as 3eV. By removing one oxygen out of 10^5 (assuming that each oxygen vacancy liberates two potentially mobile electrons), one can create a metal with a chemical potential as small as 1.1 meV on the top of this gap. It is remarkable that this can be achieved in spite of unavoidable inhomogeneities in dopant distribution. Long-range screening, which damps local band-bending effects appears to be the key factor here. This is the first major result coming out of this investigation.

This dilute liquid of electrons becomes a superconductor below a critical temperature of T_c=86 mK. This second unexpected result is illustrated in Fig. 3c, which shows the resistive transition. The width of transition (defined as the difference between the temperatures of

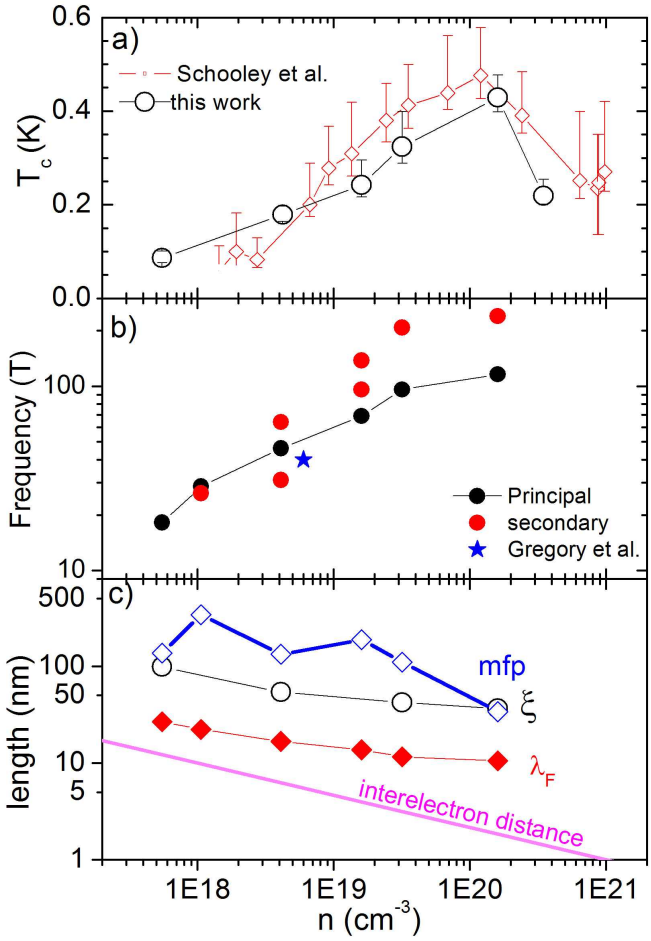

FIG. 4: **Doping dependence of the critical temperature, oscillation frequencies and various length scales: a)** Variation of the critical temperature with carrier concentration according to this work and ref.[12]. The width of superconducting transition in each case is represented by error bars. **b)** Evolution of detected frequencies as a function of doping. For carrier concentrations larger than $10^{18} cm^{-3}$, oscillations display more than one frequency. The frequency and carrier density reported in ref.[17] is also shown. **c)** Variation of four relevant length scales, namely the electronic mean-free-path, the average Fermi wavelength, λ_F of electrons of the main band, the superconducting coherence length, ξ and the interelectron distance.

10 percent and 90 percent drops in resistivity) is 25 mK. This is to be compared with a width of 30 mK in a sample with a T_c of 180 mK and a carrier density of $4.1 \times 10^{18} cm^{-3}$ (Fig. 3d). As seen in the figure, the superconducting transition is easily suppressed by the application of a small magnetic field.

Figure 4 details the evolution of superconducting and normal state properties with doping. As seen in the upper panel, the evolution of T_c with carrier concentration in our samples are comparable with those reported in ref.[12], save for the persistence of a long tail on the underdoped side of the phase diagram. The middle panel presents the evolution of frequencies resolved by quantum oscillations with carrier doping. In most samples, in addition to the main frequency, other ones were resolved pointing to the existence of several quantized orbits of electrons as successive bands are filled. For comparison, the panel shows the unique frequency previously reported in the bulk[17]. Finally, the lower panel compares the evolution of four different length scales of the system. The average interelectron distance (estimated from carrier density: $d_{ee} = n^{-1/3}$), the average Fermi wavelength (calculated from the Fermi wave-vector, k_F of the main band obtained from the principal frequency:$< \lambda_F >= \frac{2\pi}{k_F}$); the mean-free-path (estimated from the measured Hall mobility, μ_H and k_F: $\ell_e = \frac{\hbar \mu_H k_F}{e}$) and finally the superconducting coherence length (derived from the slope of the upper critical field: $\xi^{-2} = \frac{2\pi}{\Phi_0} 0.69 T_c \frac{dH_{c2}}{dT}|_{T_c}$).

Comparing these length scales, we can make several observations. With a dielectric constant as large as 2.5×10^4[9], and an effective mass of $1.8 m_e$, the Bohr radius is of the order of 0.7 μm. Therefore, the Mott criterion for metallicity ($a_B^* n^{1/3} >> 0.26$)[10] is easily satisfied. Since electrons can travel much further than the interdopant distance, the superconductor remains in the clean limit ($\ell_e > \xi$) in our range of study. Finally, the system avoids localisation, because $\ell_e >> \lambda_F$. As noted previously[23], this superconductor stays in the BCS side of the BEC-BCS cross-over. Even for the lowest concentration, the average size of Cooper pairs ($\xi \simeq 100nm$) is much longer than the interelectron distance ($d_{ee} = 12nm$).

A three-dimensional carrier density of $5.5 \times 10^{17} cm^{-3}$ corresponds to a 2D carrier density as low as $n_{2D} = 6.7 \times 10^{11} cm^{-2}$. Superconductivity at such a low carrier density has never been explored in two-dimensional $SrTiO_3$. In the interface system, the superconducting ground state is destroyed by a superconductor-to-insulator transition at higher concentrations [27]. Such a transition occurs when the condition $k_F \ell \sim 1$ is realized. In three dimensions, the mean-free-path is much longer and therefore, the threshold $k_F \ell = 1$ is pushed to much lower densities.

Thus, bulk $SrTiO_3$ offers a unique opportunity to study a dilute superconductor with a single quasi-spherical Fermi surface. Such a simple Fermi surface topology is rare among superconductors. It is a well-known fact that monovalent (noble and Alkali) metals stand

out in the periodical table by their refusal to superconduct. More importantly, the extreme low density generates several peculiar features. The Fermi velocity ($v_F = \frac{\hbar k_F}{m^*}$) becomes as low as 15 km s^{-1}, almost as slow as sound velocity. The Fermi temperature is an order of magnitude *lower* than the Debye temperature, a situation never met in a conventional superconductor, but common in a heavy-fermion superconductor. The inversion of Debye and Fermi energy scales has profound consequences for the relative weight of Coulomb repulsion and phonon-mediated attraction between electrons[28] and is a real challenge for any theory of superconductivity based on phonon-electron interaction.

Little is known about the superconducting order parameter other than the reported observation of a multi-gap superconductivity in the doping range above $10^{19} cm^{-3}$ [14]. In absence of any experimental data on the absence or presence of nodes in the gap, both the pairing mechanism and the symmetry of the order parameter remain open questions. Most theoretical scenarios for superconductivity invoke phonons as the virtual excitations exchanged by the paired electrons. Our current knowledge of Fermi surface, single-valley at the center of the Brillouin zone, leaves no room for intervalley phonons invoked by the oldest theoretical attempt to explain the existence of a superconducting dome in this system[13]. In the case of other theoretical proposals, the verdict is not as definitive. In particular, the scenario invoking the exchange of plasmons and polar optical phonons between electrons[29] appears to be comfortable with the persistence of superconductivity in a dilute one-band context.

A detailed analysis of quantum oscillations would open a new window to this issue, since it can accurately determine the density of states, $N(0)$ at arbitrary doping. Since the BCS formula ($T_c = \Theta exp[\frac{-1}{N(0)V}]$) links T_c with an energy scale Θ, an interaction parameter V and the density of states, $N(0)$, competing scenarios can be tested by comparing their expectation for the variation of V and Θ.

Acknowledgements- We acknowledge stimulating discussions with Harold Hwang, Dirk van der Marel, Kazuamasa Miyake and Yasutami Tanaka. This work is supported by Agence Nationale de la Recherche as part of QUANTHERM and SUPERFIELD projects. X.L.

acknowledges a scholarship granted by China Scholarship Council.

---

[1] Schooley J. F., Hosler W. R. and Cohen M. L., Superconductivity in Semiconducting $SrTiO_3$, *Phys. Rev. Lett.* **12**, 474–475 (1964)

[2] Hulm J. K. , Ashkin D., Deis D. W. and Jones C. K., Superconductivity in semiconductors and semimetals, *Prog. in Low Temp. Phys.* VI, 205–242 (1970)

[3] Blase X., Bustarret E., Chapelier C., Klein T., Marcenat C., Superconducting group-IV semiconductors, *Nature Materials* **8**, 375–382 (2009)

[4] Ohtomo A. and Hwang H. Y., A high-mobility electron gas at the $LaAlO_3/SrTiO_3$ heterointerface, *Nature* **427**, 423–426 (2004)

[5] Santander-Syro A. F. *et al.*, Two-dimensional electron gas with universal subbands at the surface of $SrTiO_3$, *Nature* **469**, 189–193 (2011)

[6] Reyren N. *et al.*, Superconducting Interfaces Between Insulating Oxides, *Science* **317**, 1196–1199 (2007)

[7] Biscaras J. *et al.*, Two-dimensional superconductivity at a Mott insulator/band insulator interface $LaTiO_3/SrTiO_3$, *Nature Commun.* **1**, 89 (2010)

[8] Zhu Z., Yang H., Fauqué B., Kopelevich Y. and Behnia K., Nernst effect and dimensionality in the quantum limit, *Nature Phys.* **6**, 26–29 (2010)

[9] Müller K. A. and Burkard H., $SrTiO_3$: An intrinsic quantum paraelectric below 4 K, *Phys. Rev. B* 19, 3593-3602 (1979)

[10] Edwards P. P. and Sienko M. J., Universality aspects of the metal-nonmetal transition in condensed media, *Phys. Rev. B* **17**, 2575-2581 (1978)

[11] Spinelli A. , Torija M. A., Liu C., Jan C., and Leighton C., Electronic transport in doped $SrTiO_3$: Conduction mechanisms and potential applications, *Phys. Rev. B* **81**, 155110 (2010)

[12] Schooley J. F. *et al.*, Dependence of the Superconducting Transition Temperature on Carrier Concentration in Semiconducting $SrTiO_3$, *Phys. Rev. Lett.* **14**, 305-307 (1965)

[13] Koonce C. S., Cohen M. L., Schooley J. F., Hosler W. R. , and Pfeiffer E. R., Superconducting Transition Temperatures of Semiconducting $SrTiO_3$, *Phys. Rev.* **163**, 380-390 (1967)

[14] Binnig G., Baratoff A., Hoenig H. E. and Bednorz J. G., Two-Band Superconductivity in Nb-Doped $SrTiO_3$, *Phys. Rev. Lett.* **45**, 1352-1355 (1980)

[15] Suzuki H. *et al.*, Superconductivity in Single-Crystalline $Sr_{1-x}La_xTiO_3$, *J. Phys. Soc. Jpn.* **65** 1529–1532 (1996)

[16] Frederikse H. P. R., Hosler W. R., and Thurber W. R., Babiskin J. and Siebenmann P. G., Shubnikovde Haas Effect in $SrTiO_3$, *Phys. Rev.* **158**, 775-778 (1967)

[17] Gregory B., Arthur J., and Seidel G., Measurements of the Fermi surface of $SrTiO_3$: Nb, *Phys. Rev.* **B** 19, 1039–1048 (1979)

[18] Kozuka Y., Kim M., Bell C., Kim B. G., Hikita Y. and Hwang H. Y., Two-dimensional normal-state quantum oscillations in a superconducting heterostructure, *Nature* **462**, 487-490 (2009)

[19] Ben Shalom M., Ron A., Palevski A. , and Dagan Y., Shubnikov-de Haas Oscillations in $SrTiO_3/LaAlO_3$ Interface, *Phys. Rev. Lett.* **105**, 206401 (2010)

[20] Caviglia A. D. *et al.*, Two-Dimensional Quantum Oscillations of the Conductance at $LaAlO_3/SrTiO_3$ Interfaces, *Phys. Rev. Lett.* **105**, 236802 (2010)

[21] Behnia K., Méasson M-.A. and Kopelevich Y., Oscillating Nernst-Ettingshausen Effect in Bismuth across the Quantum Limit, *Phys. Rev. Lett.* **98**, 166602 (2007).

[22] Fauqué B. *et al.*, Magnetothermoelectric properties of Bi_2Se_3, arXiv:1209.1312 (2012)

[23] van der Marel D., van Mechelen J. L. M., and Mazin I. I., Common Fermi-liquid origin of T^2 resistivity and superconductivity in n-type $SrTiO_3$, *Phys. Rev. B* **84**, 205111 (2011)

[24] Behnia K., Jaccard D. and Flouquet J., On the thermoelectricity of correlated electrons in the zero-temperature limit, *J. Phys.: Condens. Matter* **16** 5187 (2004)

[25] Okuda T., Nakanishi K., Miyasaka S., and Tokura Y., Large thermoelectric response of metallic perovskites: $Sr_{1-x}La_xTiO_3$ ($0 < x < 0.1$) *Phys. Rev. B* 63, 113104 (2001)

[26] van Mechelen J. L. M. *et al.*, Electron-Phonon Interaction and Charge Carrier Mass Enhancement in $SrTiO_3$, *Phys. Rev. Lett.* **100**, 226403 (2008)

[27] Caviglia A. D. *et al.*, Electric field control of the $LaAlO_3/SrTiO_3$ interface ground state, *Nature* **456**, 624-627 (2008)

[28] de Gennes P. G., Superconductivity of metals and alloys, W. A. Benjamin, New York (1966)

[29] Takada Y., Theory of superconductivity in polar semiconductors and its application to n-type semiconducting $SrTi0_3$, *J. Phys. Soc. Jpn.* **49** 1267–1275 (1980)